Critically-enhanced nonreciprocal electronic transport at magnetic phase boundary in a room temperature helimagnet YMn_6Sn_6

Hidetoshi Masuda [1,*] Jun-ichiro Ohe,[2] Yoichi Nii [1,†] Shojiro Kimura [1] and Yoshinori Onose [1,3]
[1]*Institute for Materials Research, Tohoku University, Sendai 980-8577, Japan*
[2]*Department of Physics, Toho University, Funabashi 274-8510, Japan*
[3]*Center for Science and Innovation in Spintronics (CSIS), Tohoku University, Sendai 980-8577, Japan*

(Received 28 December 2024; accepted 16 June 2025; published 7 July 2025)

We investigated nonreciprocal electronic transport, a diode effect of electric current flow, in a helimagnet YMn_6Sn_6. We found that nonreciprocal resistivity, whose sign depends on the handedness of the magnetic spiral (chirality), was drastically enhanced in the vicinity of the helimagnetic transition magnetic field. This critical enhancement was observed in the wide temperature range below the helimagnetic transition temperature 335 K. We comparatively discuss three possible mechanisms of nonreciprocal electronic transport: band asymmetry, current-induced deformation of the magnetic structure, and asymmetric scattering, and suggest the most plausible mechanism is the last one.

DOI: 10.1103/ltwf-zhj2

I. INTRODUCTION

Conventional magnetic storage devices utilize the direction of ferromagnetic magnetization as an information carrier [1]. Nevertheless, in the case of magnetic memory, the stray field of ferromagnets is found to be a serious problem for integration. For this reason, spintronics based on antiferromagnets has been extensively studied [2–6]. For the detection of the antiferromagnetic internal degree of freedom, in some cases, a novel response denoted as nonreciprocal electronic transport is useful. Nonreciprocal electronic transport is the rectification of the electric current in noncentrosymmetric media under a magnetic field [7–10]. If the antiferromagnetic order breaks the inversion symmetry and the spatial inversion operation interchanges two degenerated antiferromagnetic states, one can detect which state is stabilized utilizing nonreciprocal electronic transport, since the sign of the nonreciprocal resistivity is reversed by the spatial inversion operation. A unique example is a helimagnet. It is a kind of antiferromagnet in which the magnetic moments are within a plane perpendicular to the propagation vector, and the in-plane angle gradually increases along the propagation vector to construct a spiral. Two rotational directions of the magnetic spiral (chirality) are transformed into each other by spatial inversion. Recent experiments showed that chirality can be detected by nonreciprocal electronic transport [11,12].

There are three possible mechanisms of nonreciprocal transport in a helimagnet, as shown in Fig. 1. The first mechanism is the electronic band asymmetry in the momentum space. For example, in noncentrosymmetric semiconductors [13,14], spin-orbit-driven spin-splitting such as the Rashba and Dresselhaus effects, combined with the Zeeman effect under magnetic fields, gives rise to the asymmetric band structure in momentum space, which is the origin of nonreciprocal electronic transport in these materials. Because helimagnets also show similar splitting [15], this mechanism of nonreciprocal electronic transport seems to apply to helimagnets, as shown in Fig. 1(a) [16]. The second mechanism is the current-induced deformation of the helimagnetic structure. In the conical magnetic state under a magnetic field along the propagation vector, an electric current j additionally applied parallel or antiparallel to the magnetic field changes the tilting angle of the conical magnetic structure depending on the chirality and the relative configuration (parallel or antiparallel) of the magnetic field and electric current, as shown in Fig. 1(b). In one chirality, the electric current parallel (antiparallel) to the magnetic field increases (decreases) the conical angle and the net magnetization. In the other chirality, the sign of the current-induced magnetization change is the opposite. Because the resistivity should, more or less, reflect the change in the conical angle, the resistivity depends on the sign of the electric current. The third mechanism is asymmetric scattering. When the rate of scattering from momentum $+k$ to $-k$ is different from that of $-k$ to $+k$, the electronic transport becomes nonreciprocal. Researchers have reported that spin-momentum locking in noncentrosymmetric systems makes the scattering by ferromagnetic objects asymmetric [17]. Because the helimagnetic structure also induces spin-momentum locking, as shown in Fig. 1(a), asymmetric scattering is expected by the ferromagnetic fluctuation in the helimagnetic state [Fig. 1(c)].

In this paper, we studied nonreciprocal electronic transport in a helimagnet YMn_6Sn_6. We found that nonreciprocal resistivity is critically enhanced at the helimagnetic phase boundary. We comparatively discussed the three mechanisms

*Contact author: hidetoshi.masuda.c8@tohoku.ac.jp
†Present address: Department of Applied Physics and Physico-Informatics, Keio University, Yokohama 223-8522, Japan.

Published by the American Physical Society under the terms of the Creative Commons Attribution 4.0 International license. Further distribution of this work must maintain attribution to the author(s) and the published article's title, journal citation, and DOI.

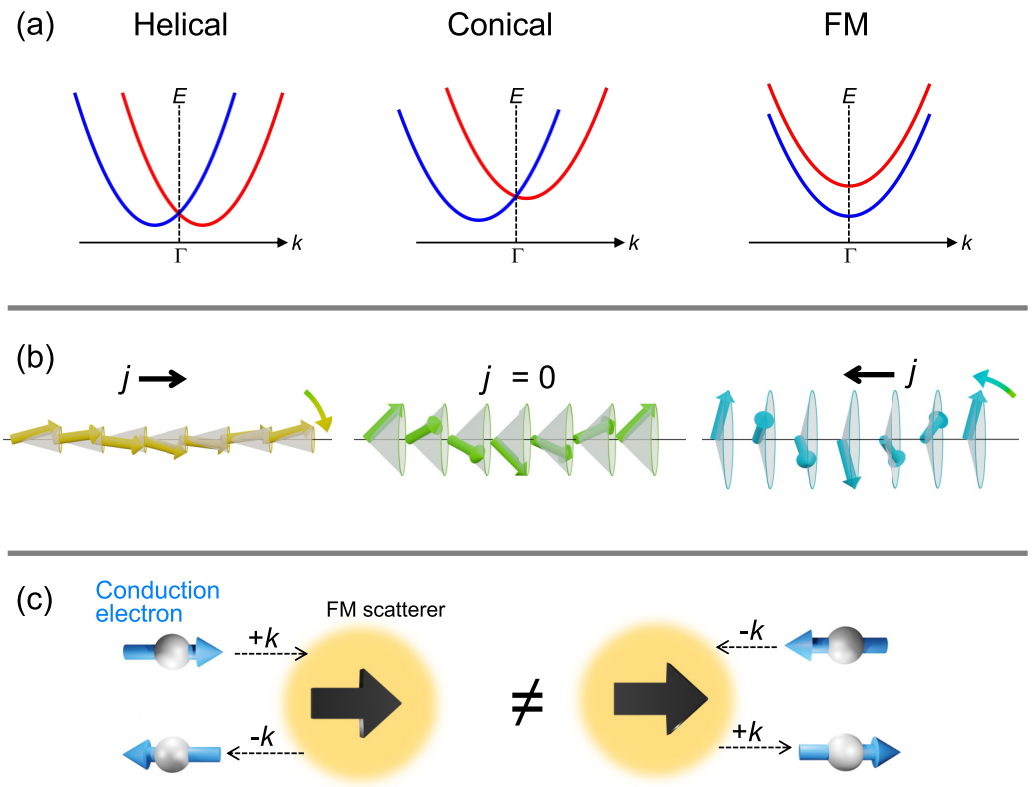


FIG. 1. Schematic illustration of three possible mechanisms for nonreciprocal electronic transport in a helical magnet. (a) Band asymmetry mechanism. In the conical state, the electronic band dispersion acquires asymmetry due to the $s-d$ exchange interaction, leading to nonreciprocal electronic transport. (b) Current-induced deformation of magnetic structure. In a magnetic field along the helical propagation vector, the conical magnetic structure is stabilized. When an electric current is applied parallel or antiparallel to the magnetic field, the conical angle increases or decreases, depending on the chirality and signs of the electric current and magnetic field. This leads to the nonreciprocal electronic transport. (c) Asymmetric scattering by the ferromagnetic object. Due to spin-momentum locking, the electron scattering by ferromagnetic cluster or fluctuation is asymmetric in a helimagnetic state, leading to nonreciprocal electronic transport.

of nonreciprocal electronic transport and found that asymmetric scattering is the most plausible.

II. RESULTS AND DISCUSSION

YMn_6Sn_6 has a centrosymmetric hexagonal crystal structure with the space group $P6/mmm$, as shown in Fig. 2(a). The Mn magnetic moments show a colinear antiferromagnetic order between 335 K and 345 K and a helimagnetic order below 335 K. The helimagnetic propagation vector is (0,0,0.27) in the reciprocal lattice unit at 200 K [18,19]. See Supplemental Material Fig. S1 for the temperature dependence of the magnetization and resistivity [20]. Similar magnetic transitions were observed in the course of magnetic field application at a low temperature. Figure 2(c) shows the magnetization curve for $H \parallel c$ at 200 K. Magnetization M shows two anomalies at $H_c = 7.6$ T and $H_{c'} = 8.0$ T, and tends to saturate at higher fields. Based on the continuity of the transition fields in the temperature-field phase diagram ([see Fig. 4(a)], two anomalies can be attributed to the transition field from the helical phase to the antiferromagnetic phase, and that from the antiferromagnetic phase to the induced ferromagnetic phase. Figure 2(d) shows the H dependence of the normalized magnetoresistance $(\rho(H) - \rho(0))/\rho(0)$ for $j \parallel H \parallel c$ at 200 K. Here, the resistivity ρ was measured for a micrometer-sized Hall bar device with a cross-sectional area of $\sim 1 \times 1$ μm^3 fabricated by the focused-ion beam technique [see Fig. 2(b) and the Supplemental Material for the fabrication process and characterization]. ρ decreases monotonically on increasing magnetic field, accompanied by an anomaly at 7.4 T, which can be attributed to the helimagnetic transition field H_c. The slightly lower transition field seems to be caused by the microfabrication.

The nonreciprocal electronic transport can be estimated from the second-harmonic ac resistivity $\rho^{2\omega}$ [13]. Since the nonreciprocal resistivity is odd in time-reversal operation, the field-asymmetric component $\rho^{2\omega}_{\rm asym}(H) = (\rho^{2\omega}(+H) - \rho^{2\omega}(-H))/2$ is regarded as the nonreciprocal resistivity. The raw data for $\rho^{2\omega}$ are shown in the Supplemental Material [20]. The sign of $\rho^{2\omega}_{\rm asym}$ is defined to be opposite to that of $\Delta\rho_{\rm asym}$, field asymmetric component of $\Delta\rho = (\rho(+j_{\rm dc}) - \rho(-j_{\rm dc}))/2$, where $\rho(\pm j_{\rm dc})$ is the resistivity measured with positive and negative dc current $\pm j_{\rm dc}$. We also measured $\Delta\rho_{\rm asym}$ and confirmed the sign definition [see the inset of Fig. 2(e) and Supplemental Material Sec. VI]. Before measuring the nonreciprocal resistivity, we controlled the helimagnetic chirality in our microfabricated device in a manner similar to Refs. [11,12,21]. We swept the magnetic field from H_0 ($|H_0| > H_c$) to 0 T with the application of dc electric current j_0 ($j_0 = 0, \pm 8.0 \times 10^8$ A/m^2), so that the chirality is controlled depending on whether the magnetic field and

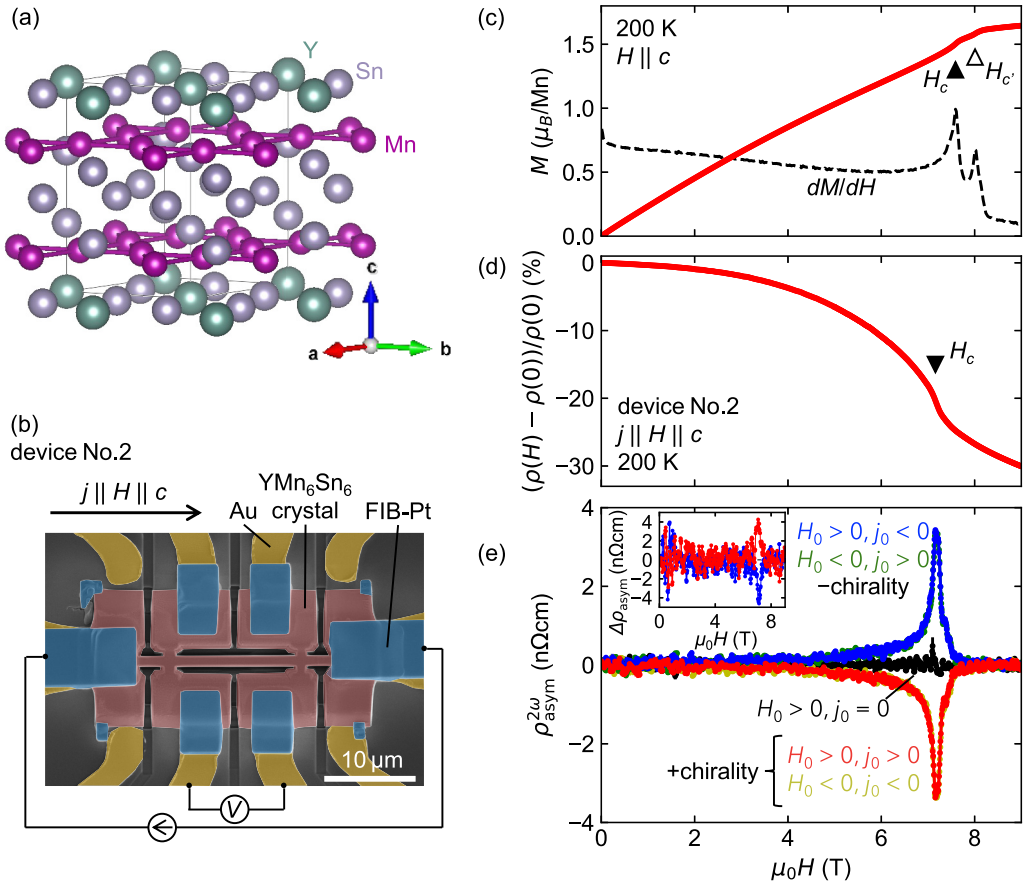


FIG. 2. (a) Crystal structure of YMn_6Sn_6 drawn using VESTA [24]. (b) Scanning electron microscope image of the focused ion beam (FIB) microfabricated device No. 2. The YMn_6Sn_6 crystal was shaped into a Hall bar by means of FIB microfabrication. Electric current passes through the thin horizontal bar along the c axis, and the voltage drop is measured between two vertical bars. (c) Magnetic field H dependence of the magnetization M at 200 K. Closed and open triangles denote the transition field from the helimagnetic to the antiferromagnetic phase (H_c) and that from the antiferromagnetic to the induced-ferromagnetic phase ($H_{c'}$), respectively. (d) H dependence of the normalized magnetoresistance $(\rho(H) - \rho(0))/\rho(0)$. A closed triangle denotes H_c. (e) H dependence of the nonreciprocal resistivity $\rho^{2\omega}_{\rm asym}$. Before the measurements, the helimagnetic chirality was controlled by the magnetic field sweep from $H_0 = \pm 9$ T to 0 T with the application of dc electric current $j_0 = 0, \pm 8.0 \times 10^8$ A/m^2. The measurements of nonreciprocal resistivity were performed using the ac electric current with an amplitude of $j_{\rm ac} = 1.5 \times 10^8$ A/m^2. Inset shows $\Delta\rho_{\rm asym}$, the field asymmetric component of $\Delta\rho = (\rho(+j_{\rm dc}) - \rho(-j_{\rm dc}))/2$, for $H_0 > 0$, $j_0 > 0$ (red) and $H_0 > 0$, $j_0 < 0$ (blue), which confirms the sign of $\rho^{2\omega}_{\rm asym}$ is opposite to that of $\Delta\rho_{\rm asym}$ (see the Supplemental Material for the measurement details [20]).

electric current are parallel ($H_0 j_0 > 0$) or antiparallel ($H_0 j_0 < 0$) to each other. For $j_0 = 0$, the chirality should be equally distributed. After the chirality control, we turned off the dc current j_0 and alternatively applied an ac current $j_{\rm ac}$ to measure $\rho^{2\omega}$. We separately measured $\rho^{2\omega}$ on increasing the magnetic field from 0 T to +9 T and that on decreasing the magnetic field from 0 T to −9 T just after the chirality controls, and calculated $\rho^{2\omega}_{\rm asym}(H) = (\rho^{2\omega}(+H) - \rho^{2\omega}(-H))/2$.

Figure 2(e) shows the H dependence of the nonreciprocal resistivity $\rho^{2\omega}_{\rm asym}$ measured after the chirality-control procedure with $H_0 = \pm 9$ T and $j_0 = 0, \pm 8.0$ A/m^2 for $j \parallel H \parallel c$ at 200 K. While $\rho^{2\omega}_{\rm asym}$ was negligibly small for $j_0 = 0$, we identified distinct $\rho^{2\omega}_{\rm asym}$ depending on the sign of $H_0 j_0$, confirming the chirality control by the magnetic field sweep with the dc electric current. The chirality dependence cannot be explained by the Joule heating effect. See the Supplemental Material [20] for the j_0 and $j_{\rm ac}$ dependence. $\rho^{2\omega}_{\rm asym}$ shows a unique magnetic field dependence. It is vanishingly small at low fields below 5 T. However, it steeply increases toward the helimagnetic transition field H_c, and then suddenly vanishes above H_c, showing a prominent peak-like feature at H_c. The sharp peak at H_c was not observed in other helimagnets having centrosymmetric crystal structures [11,12,16].

Figure 3 shows the H dependence of $\rho^{2\omega}_{\rm asym}$ at various temperatures. We note that the measurements are performed on two devices: device No. 1 measured between 240 K and 340 K, and device No. 2 between 75 K and 300 K. The data for the two devices are consistent in the overlapping temperature region. See the Supplemental Material [20] for the data on device No. 3 measured between 5 K and 200 K. The nonreciprocal resistivity vanishes above the helimagnetic transition temperature $T_c = 335$ K, being consistent with the helimagnetic origin of the nonreciprocal electronic transport. Nonzero $\rho^{2\omega}_{\rm asym}$ with prominent peak-like features at H_c were observed at all temperatures below T_c. Figure 4(b) shows the temper-

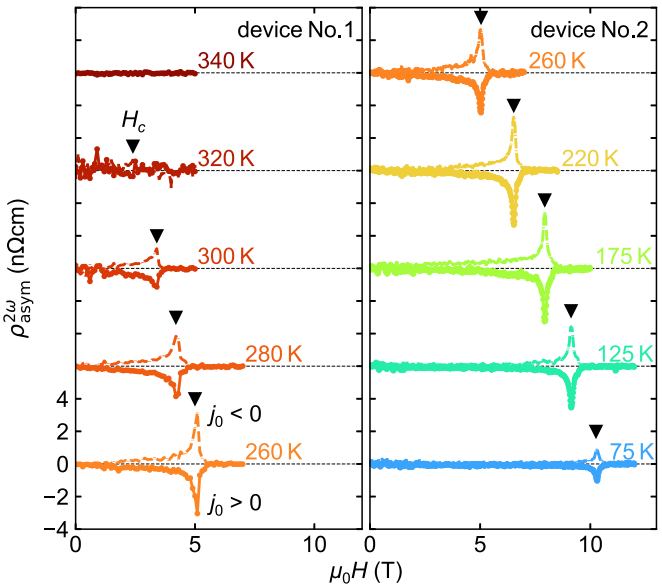


FIG. 3. H dependence of $\rho^{2\omega}_{asym}$ at selected temperatures. Data were measured after the chirality control by the magnetic field sweep from H_0 ($H_0 > H_c$) with the application of dc electric current $j_0 = \pm 8.0 \times 10^9$ A/m^2 at each temperature. Triangles denote H_c estimated from the magnetoresistance. Data were measured for two different devices in the different temperature regions: device No. 1 was measured in the region of 240–340 K and device No. 2 in 75–300 K. Data for device No. 3 measured in 5–200 K are shown in the Supplemental Material [20].

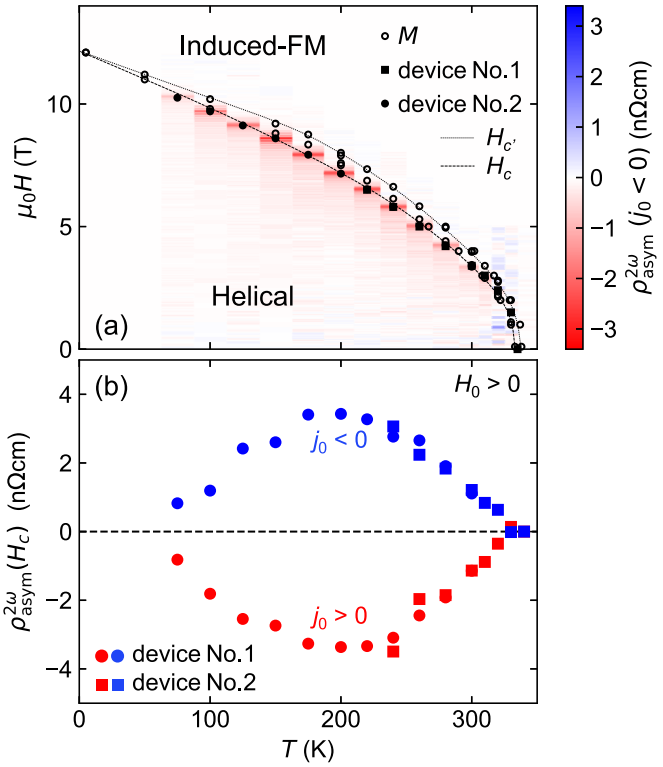


FIG. 4. (a) Contour plot of $\rho^{2\omega}_{asym}$ for $j_0 < 0$ in the $H - T$ plane for $H \parallel c$. Open black circles denote H_c and $H_{c'}$ estimated from the magnetization. Filled black circles and squares denote H_c determined from magnetoresistance for devices No. 1 and No. 2, respectively. Dashed and dotted lines are guides for the eye. Induced-FM denotes the induced ferromagnetic state. (b) Temperature T dependence of the nonreciprocal resistivity $\rho^{2\omega}_{asym}$ at $H = H_c$. Squares and circles denote the data measured on devices No. 1 and No. 2, respectively.

ature dependence of $\rho^{2\omega}_{asym}$ at $H = H_c$. Below T_c, it gradually increases and shows a broad maximum around 200 K, and slowly decreases toward the lowest temperature. Figure 4(a) is the contour plot of $\rho^{2\omega}_{asym}$ in the temperature-magnetic field phase diagram. It is clear from this figure that $\rho^{2\omega}_{asym}$ is critically enhanced at the helimagnetic phase boundary.

Then, let us consider the mechanism of the observed nonreciprocal electronic transport. The asymmetry in band structure is considered to be the main origin of nonreciprocal electronic transport in noncentrosymmetric semiconductors [13,14]. The conical magnetic structure can also induce band asymmetry through exchange splitting [15] [see Fig. 1(a) and Fig. S12 in the Supplemental Material [20], which gives rise to nonreciprocal electronic transport as reported recently [16]. To investigate whether this mechanism is responsible for the nonreciprocal electronic transport in YMn_6Sn_6, we calculated the nonreciprocal resistivity arising from the band asymmetry in the conical magnetic state by using the Boltzmann equation and compared its magnetic field dependence to that observed in YMn_6Sn_6 (see the Supplemental Material [20] for calculation details). Calculated nonreciprocal resistivity shows a broad maximum at $H/H_c \sim 0.5$, and smoothly decreases to zero at H_c, which is clearly distinct from the experimental observation. Another mechanism is the current-induced conical deformation mechanism shown in Fig. 1(b). As mentioned, the conical magnetization M is changed by the application of electric current j. The resistivity ρ under j is expressed as

$$\rho(j) \simeq \rho_0 + \frac{d\rho}{dH}\left(\frac{dM}{dH}\right)^{-1}\Delta M, \qquad (1)$$

where ρ_0 and ΔM are the linear resistivity and the current-induced magnetization change, respectively. When $\Delta M \propto j$, the second term explains the nonreciprocal electronic transport. Nevertheless, the expected sign of the nonreciprocal resistivity in this mechanism is opposite to the observed one, while the magnitude is expected to be enhanced at the helimagnetic critical field according to numerical calculation, as shown in the Supplemental Material [20]. For this reason, we concluded that it cannot explain the experimental observation.

Therefore, the asymmetric scattering mechanism seems to be the most plausible scenario. Recently, Ishizuka and Nagaosa suggested that scattering by the chiral magnetic cluster is asymmetric and induces nonreciprocal transport in the ferromagnetic state [22]. We found that scattering by a ferromagnetic cluster is also asymmetric in the helimagnetic state, as shown in Fig. 1(c). When the conduction electrons are coupled to the helimagnetic localized moments by the exchange interaction, the spin and momentum of conduction electrons along the helimagnetic propagation vector are locked to each other, as shown in Fig. S12 in the Supplemental Material [20]. Assuming the helimagnetic propagation vector is along the z-axis, the electronic states with momentum $(0, 0, +k)$ and $(0, 0, -k)$ have positive and negative spin moments along the z-axis in a chiral state. When the angular momentum is preserved in the course of scattering by the ferromagnetic

cluster, the scattering from $(0, 0, +k)$ to $(0, 0, -k)$ transfers the positive angular momentum from the conduction electron to the cluster, and that from $(0, 0, -k)$ to $(0, 0, +k)$ does the negative angular momentum. When the ferromagnetic moment is fully polarized along the positive z-direction, the former scattering should be forbidden while the latter is allowed. In that way, the scattering by the ferromagnetic cluster becomes asymmetric. Of course, there is not a completely static ferromagnetic cluster in a helimagnetic state, but the ferromagnetic fluctuation should exist in the vicinity of the phase boundary to the ferromagnetic state. The observed nonreciprocal electronic transport is critically enhanced at the phase boundary, and therefore, we ascribed the origin to asymmetric scattering. The temperature dependence of nonreciprocal resistivity also seems to be explained based on the asymmetric scattering scenario. Because the magnetic fluctuation is expected to increase with temperature, the scattering magnitude is also expected to increase with temperature. Nevertheless, the helimagnetic structure gradually weakens as the temperature increases toward the transition temperature. The temperature dependence seems to be determined by the competition. Nevertheless, it should be noted that the argument is quite simplified, and in particular, we ignore the antiferromagnetic state between the helimagnetic and ferromagnetic states. Perhaps, the quasistatic antiferromagnetic fluctuation is nearly polarized in high magnetic fields, and the scattering may be antisymmetric, inducing nonreciprocal electronic transport. For quantitative discussion, a more elaborate theory is needed.

III. CONCLUSION

In summary, we investigated nonreciprocal electronic transport in a helimagnet YMn_6Sn_6. The nonreciprocal resistivity, which sensitively probes the chirality controlled by an electric current and a magnetic field, shows a singular enhancement in the vicinity of the helimagnetic transition field. Because the band-asymmetry mechanism and the current-induced deformation of magnetic structure cannot explain the observed nonreciprocal resistivity, we ascribed the origin to asymmetric scattering. The spin-momentum locking in the helimagnetic state appears to induce asymmetry in the scattering process and nonreciprocal electronic transport. We found that a similar mechanism also seems to work in another helimagnet, MnP, in which some of the present authors reported nonreciprocal electronic transport [11]. In that material, there is a first-order phase transition from the high-temperature ferromagnetic state to the low-temperature helimagnetic state, and nonreciprocal electronic transport was observed just around the phase boundary. One of the mysteries of nonreciprocal electronic transport in that material was that the magnetic field dependence was similar to that of ferromagnetic magnetization. Assuming that the nonreciprocal electronic transport was induced by the asymmetric scattering from the ferromagnetic cluster, the magnetic field dependence was naturally understood. This indicates that nonreciprocal electronic transport should be enhanced even in the low field in helimagnet-ferromagnet composite materials, which could be useful for future applications. This is different from the conclusion of our recent paper studying another helimagnet, α-EuP_3, in which we ascribed the origin of nonreciprocal electronic transport to the band asymmetry [16]. The nonreciprocal resistivity in helimagnets appears to be dependent on the materials. The magnitude of band asymmetry is caused by the spin splitting due to helimagnetic structure, but the magnitude of asymmetry should depend on the original band structure. Current-induced magnetization change is universally realized in helimagnets, but the magnitude depends on magnetic anisotropy and damping constants. The asymmetric scattering magnitude is dependent on the critical fluctuation at the phase boundary. Material dependence in helimagnets must be investigated further to establish a comprehensive understanding of nonreciprocal electronic transport in helimagnets.

Note that while this paper was being reviewed, another paper presenting nonreciprocal electronic transport in YMn_6Sn_6 was published [23]. Nevertheless, the scope differs from the present paper. The previously published paper mainly discusses nonreciprocal electronic transport in the conflagration of $H \perp j$, while the present paper shows the detailed magnetic field and temperature dependences of nonreciprocal resistivity in the configuration of $H||j$.

ACKNOWLEDGMENTS

The authors thank Y. Kodama and T. J. Konno for their technical assistance in using the FIB technique. This work was partially supported by JSPS (KAKENHI No. JP22H00101, No. JP23H04863, No. JP23K13654, No. JP23K17660, No. JP23K20821, No. JP24H01638, No. JP24H00189, No. JP24K01283, No. JP24K21725) and JST (PRESTO No. JPMJPR245A and FOREST No. JPMJFR2133). This study was partially supported by the Center for Integrated Nano Technology Support, Tohoku University in MEXT Advanced Research Infrastructure for Materials and Nanotechnology in Japan (JPMXP1224TU0118), and the GIMRT Program of the Institute for Materials Research, Tohoku University (Proposals No. 202412-CRKEQ-0402 and No. 202308-HMKPA-0421).

DATA AVAILABILITY

The data that support the findings of this article are not publicly available. They are available from the authors upon reasonable request.

[1] B. Dieny, R. B. Goldfarb, and K.-J. Lee, *Introduction to Magnetic Random-Access Memory* (Wiley-IEEE Press, Hoboken, NJ, 2016).

[2] A. H. MacDonald and M. Tsoi, Antiferromagnetic metal spintronics, Philos. Trans. R. Soc. A **369**, 3098 (2011).

[3] E. V. Gomonay and V. M. Loktev, Spintronics of antiferromagnetic systems (Review article), Low Temp. Phys. **40**, 17 (2014).

[4] T. Jungwirth, X. Marti, P. Wadley, and J. Wunderlich, Antiferromagnetic spintronics, Nat. Nanotechnol. **11**, 231 (2016).

[5] V. Baltz, A. Manchon, M. Tsoi, T. Moriyama, T. Ono, and Y. Tserkovnyak, Antiferromagnetic spintronics, Rev. Mod. Phys. **90**, 015005 (2018).

[6] L. Šmejkal, J. Sinova, and T. Jungwirth, Emerging research landscape of altermagnetism, Phys. Rev. X **12**, 040501 (2022).

[7] G. L. J. A. Rikken, J. Fölling, and P. Wyder, Electrical magnetochiral anisotropy, Phys. Rev. Lett. **87**, 236602 (2001).

[8] G. L. J. A. Rikken and P. Wyder, Magnetoelectric anisotropy in diffusive transport, Phys. Rev. Lett. **94**, 016601 (2005).

[9] F. Pop, P. Auban-Senzier, E. Canadell, G. L. J. A. Rikken, and N. Avarvari, Electrical magnetochiral anisotropy in a bulk chiral molecular conductor, Nat. Commun. **5**, 3757 (2014).

[10] Y. Tokura and N. Nagaosa, Nonreciprocal responses from non-centrosymmetric quantum materials, Nat. Commun. **9**, 3740 (2018).

[11] N. Jiang, Y. Nii, H. Arisawa, E. Saitoh, and Y. Onose, Electric current control of spin helicity in an itinerant helimagnet, Nat. Commun. **11**, 1601 (2020).

[12] H. Masuda, T. Seki, J.-i. Ohe, Y. Nii, H. Masuda, K. Takanashi, and Y. Onose, Room temperature chirality switching and detection in a helimagnetic $MnAu_2$ thin film, Nat. Commun. **15**, 1999 (2024).

[13] T. Ideue, K. Hamamoto, S. Koshikawa, M. Ezawa, S. Shimizu, Y. Kaneko, Y. Tokura, N. Nagaosa, and Y. Iwasa, Bulk rectification effect in a polar semiconductor, Nat. Phys. **13**, 578 (2017).

[14] G. L. J. A. Rikken and N. Avarvari, Strong electrical magnetochiral anisotropy in tellurium, Phys. Rev. B **99**, 245153 (2019).

[15] A. Zadorozhnyi and Y. Dahnovsky, Anomalous Hall effect in conical helimagnetic crystals, Phys. Rev. B **107**, 035202 (2023).

[16] A. H. Mayo, D.-A. Deaconu, H. Masuda, Y. Nii, H. Takahashi, R. V. Belosludov, S. Ishiwata, M. S. Bahramy, and Y. Onose, Band asymmetry-driven nonreciprocal electronic transport in a helimagnetic semimetal α-EuP_3, Proc. Natl. Acad. Sci. USA **122**, e2405839122 (2025).

[17] K. Yasuda, A. Tsukazaki, R. Yoshimi, K. S. Takahashi, M. Kawasaki, and Y. Tokura, Large unidirectional magnetoresistance in a magnetic topological insulator, Phys. Rev. Lett. **117**, 127202 (2016).

[18] G. Venturini, D. Fruchart, and B. Malaman, Incommensurate magnetic structures of RMn_6Sn_6(R = Sc, Y, Lu) compounds from neutron diffraction study, J. Alloys Compd. **236**, 102 (1996).

[19] N. J. Ghimire, R. L. Dally, L. Poudel, D. C. Jones, D. Michel, N. T. Magar, M. Bleuel, M. A. McGuire, J. S. Jiang, J. F. Mitchell, J. W. Lynn, and I. I. Mazin, Competing magnetic phases and fluctuation-driven scalar spin chirality in the kagome metal YMn_6Sn_6, Sci. Adv. **6**, eabe2680 (2020).

[20] See Supplemental Material at http://link.aps.org/supplemental/10.1103/ltwf-zhj2 for a description of the experimental methods, theoretical calculations, and supplemental data.

[21] J.-i. Ohe and Y. Onose, Chirality control of the spin structure in monoaxial helimagnets by charge current, Appl. Phys. Lett. **118**, 042407 (2021).

[22] H. Ishizuka and N. Nagaosa, Anomalous electrical magnetochiral effect by chiral spin-cluster scattering, Nat. Commun. **11**, 2986 (2020).

[23] D. Yamaguchi, A. Kitaori, N. Nagaosa, and Y. Tokura, Current control of spin helicity and nonreciprocal charge transport in a multiferroic conductor, Adv. Mater. **37**, 2420614 (2025).

[24] K. Momma and F. Izumi, *VESTA3* for three-dimensional visualization of crystal, volumetric and morphology data, J. Appl. Crystallogr. **44**, 1272 (2011).